Solubilization and Phase Equilibria of Water-in-Oil Microemulsions

II. Effects of Alcohols, Oils, and Salinity on Single-Chain Surfactant Systems

ROGER LEUNG AND DINESH O. SHAH

Center for Surface Science and Engineering and Departments of Chemical Engineering and Anesthesiology, University of Florida, Gainesville, Florida 32611

Received August 19, 1986; accepted February 6, 1987

The solubilization and phase equilibria of water-in-oil (w/o) microemulsions have been studied to elucidate how the molecular structure of various components of microemulsions and salinity influence two interfacial parameters of the system, namely the spontaneous curvature and elasticity of interfacial films. Most solubilization and phase equilibria data presented are explained by the change of these two parameters. It is indicated that oil can influence the property of an interfacial film by a solvation effect. Oil molecules with small molecular volume or high aromaticity produce a strong solvation effect and consequently lead to a greater penetration of oil molecules into the surfactant chain layer, thus increasing the rigidity and curvature of the interface. The addition of alcohol exhibits strong effects on the elasticity and spontaneous curvature of an interface. Decreasing alcohol chain length can increase the fluidity of the interfacial film and hence increase the attractive interdroplet interaction. On the other hand, increasing alcohol chain length often increases the rigidity and curvature of an interface. For alcohols which increase the interfacial fluidity, increasing alcohol partitioning at the interface will increase the fluidity and natural radius of the interface. The addition of electrolytes results in tighter molecular packing at the interface and a decrease in the natural radius and interfacial fluidity. There often exists an optimal salinity for a given w/o microemulsion system at which a maximum brine solubilization occurs. The maximum solubilization is interpreted as a result of counteracting effects of attractive interdroplet interaction of fluid interfaces and the bending stress of rigid interfaces. As a result of this study, phenomenological guidelines for the formulation of microemulsions have been proposed. It is inferred that the addition of a small amount of alcohol at optimal salinity together with the condition of chain length compatibility can result in the largest possible brine solubilization in a given w/o microemulsion.

INTRODUCTION

In the previous part of this series, basic concepts and theory about solubilization and phase equilibria of water-in-oil microemulsions were presented. It was shown that the solubilization and phase equilibria of w/o microemulsions can be basically accounted for by two phenomenological parameters of the system, namely the spontaneous curvature and elasticity of interfacial films. In this paper, we present some experimental results to verify and elucidate the proposed theory, and to further delineate the influence of the molecular structure of various components of microemulsions on the spontaneous curvature and elasticity of interfaces. We shall further discuss the observation of a chain length compatibility effect in w/o microemulsions (1, 2). As a result of this study, some phenomenological guidelines for the formulation of microemulsions will be proposed.

MATERIALS AND METHODS

Sodium stearate (LOT-CC-6581) was used as supplied by ICN Pharmaceuticals. Sodium dodecyl sulfate (SDS) was purchased from BDH (purity ~ 99%). All alcohols and oils with purity above 99% were used directly without further purification.

The solubilization limit of microemulsions was determined by titration of microemulsions with water or brine under ambient conditions

0021-9797/87 $3.00

until opaqueness occurred. The onset of opaqueness was defined as the turbid, milky appearance of a system such that nothing can be seen through it. The bluish, translucent appearance of a system (Rayleigh scattering) was not considered as the onset of opaqueness. However, for the transition of isotropic microemulsions to a birefringent phase, the boundary was determined as the onset of cloudiness due to a lack of strong turbidity. The reproducibility of titration was within ±0.1 ml. Birefringence was detected by viewing the sample through two cross-polarized plates.

The results of phase equilibria of samples were recorded after 48 h equilibration under ambient conditions. This equilibration period was found to be sufficient for qualitative determination of the type of phase equilibria, although true thermodynamic equilibrium may require a longer time. The type of phase equilibrium of a sample is represented by a letter beside each data point in all figures as follows.

i. Phase equilibria of microemulsions with excess water (referred as type 1 phase equilibria) are labeled "w." Phase separation of this type is due to the interfacial bending stress of rigid interfaces.

ii. Phase equilibria of microemulsions with excess oil containing a low density of microemulsion droplets are labeled "o" (referred as type 2 phase equilibria). A critical point at which two equal-volume, isotropic phases are in equilibrium is labeled "o_c." Phase separation of this type is associated with attractive interactions of fluid interfaces.

iii. A transition from an isotropic microemulsion to a birefringent phase is labeled "b."

iv. The existence of "gel-like" or solid surfactant precipitates swollen by water is labeled "p."

v. A special symbol "ô" has been used to designate the phase equilibria of microemulsions with excess oil in the second isotropic region (see text in Section I. 2) where the microemulsion structure is uncertain.

RESULTS AND DISCUSSIONS

I. Effect of Oil Chain Length

1. Influence of oil penetration into interfacial films. The water solubilization and phase equilibria of w/o sodium stearate microemulsions as a function of oil chain length are shown in Fig. 1a. The change of the electrical resistance of these solutions as a function of water concentration has been reported in Ref. (1). The result suggests that the structure of these samples is likely to be a percolating w/o microemulsion (3). The amount of solubilized water in the microemulsions increases with increasing oil chain length up to dodecane, and then decreases upon further increasing the oil chain length. The condition of "chain length compatibility" would predict a maximum solubilization at tridecane (1). Furthermore, the phase separation of microemulsions exhibits distinct patterns with varying oil chain length. For oils longer than dodecane, an isotropic microemulsion phase in equilibrium with an excess oil phase (type 2) was observed, indicating an attractive interaction between droplets for phase separation. For oils shorter than dodecane, a birefringent liquid crystalline phase was observed between dodecane and octane. Figure 7 in Ref. (1) best depicts the patterns of the observed phase equilibria. For oils shorter than octane, solid or gel-like surfactant precipitates were observed. We have calculated the equivalent alkane carbon number (EACN) of benzene to be 2.4 based on an extrapolation of solubilization data of octane, hexane, and pentane in Fig. 1a using a second-order equation. Although the EACN of benzene may vary with the composition of microemulsions, we shall always report benzene as an oil with a carbon number of 2.4 throughout this paper for convenience.

The decrease in water solubilization in microemulsions with increasing oil chain length (C_{12} to C_{16}) in Fig. 1a can be attributed to the enhanced interdroplet attraction according to the theory presented in part I. It has been experimentally established that the attractive in-

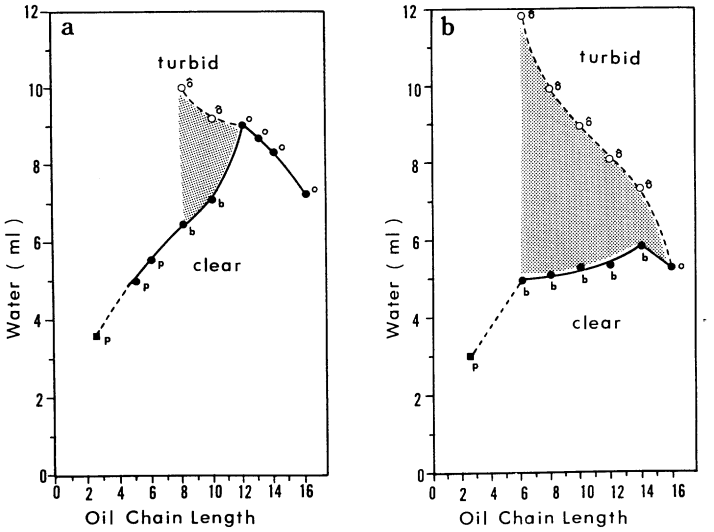

FIG. 1. Solubilization of water as a function of oil chain length in the microemulsions containing 10 ml oil, 1 g sodium stearate, and various amounts of 1-pentanol: 8 ml (a) and 4 ml (b). The filled circles stand for the first boundary, while the open circles represent the second boundary of solubilization. Benzene is plotted as an oil with a chain length of 2.4 (filled square) and the screened area indicates a clear birefringent region. Each letter beside the data points represents the type of phase equilibrium of each sample. See text for other details.

teraction between w/o microemulsion droplets increases with increasing oil chain length (4–7). This enhanced attraction is related to the penetration of oil molecules into the interfacial film, and the resultant change in interfacial curvature and fluidity. Many experimental and theoretical studies of microemulsions (8–10) and amphiphilic bilayers (11–16) have suggested that oil penetration into interfacial films increases with decreasing molecular volume and the increasing aromaticity of the oil. This penetration can increase the interfacial mixing entropy, thus stabilizing the interfacial film. The oil penetration also swells the aliphatic layer of the surfactant film, causing a higher spreading pressure at the surfactant tail/oil interface, and consequently resulting in a more curved interface (smaller droplet size). Further, the oil penetration straightens the surfactant chain (favors transconformation of the chain) and consequently leads to a more rigid, hardened interfacial film (8, 10, 12, 15–17). All these factors serve as stabilizing forces for w/o microemulsion droplets (17). In contrast, less penetration of oil into the surfactant film with increasing oil chain length results in a more flexible interface and a greater natural radius (R_0) than that of short-chain oils. The attractive interactions between droplets are thus increased due to "sticky" collisions between droplets (18, 19) and a decrease in interfacial bending energy upon the formation of dimers (20). The "stickiness" of collisions is proportional to the fluidity of the interface, the thickness and the area of the penetrable aliphatic layer (21–23), and the ease of oil removal from the interface upon collisions (23). The last factor is very similar to the case of steric stabilization in polymeric colloidal systems (24, 25). One can consider the long-chain oil as a "poor" solvent for interfacial films, resulting in attractive steric forces between microemulsion droplets in analogy to that between polymer-coated particles (24, 25).

2. Formation of birefringent phases. As shown in Fig. 1a, the water solubilization in the microemulsions diminishes as the oil chain length decreases from dodecane to octane. An

unusual phase transition of isotropic → birefringent → isotropic → turbid was observed when water was continuously added to the solution. A similar phase transition has also been reported in other w/o microemulsion systems (26–30). The birefringent phase appears translucent and consists of a fine liquid crystalline dispersion, analogous to a neat phase in equilibrium with the L_2 phase in many lyotropic liquid crystalline systems (31). Ekwall (31) has indicated that a neat phase (lamellae) often occurs when the solubilization limit of an isotropic w/o microemulsion phase (L_2) is exceeded. The "second" isotropic phase at a higher water content appears bluish and translucent and has a very narrow water solubilization range as compared to the "first" isotropic phase or the birefringent phase. We shall refer to the transition of the second isotropic to turbid phase as the "second boundary" in contrast to the "first boundary" of transition from the first isotropic to birefringent phase.

A possible structure of o/w microemulsions has been suggested for some second isotropic phases (26). However, a similar second isotropic region observed in AOT systems (30) indicates that the second isotropic region connects with the L_2 (w/o) phase through a narrow passage. The exact nature and structure of this second isotropic phase probably still remains to be studied. One possibility is that the second isotropic phase in Fig. 1a represents a gradual and continuous phase inversion from w/o to o/w droplets, as moving from dodecane to octane.

In an attempt to delineate the relation between a microemulsion and a lyotropic nematic phase, specific lamellar phases have been studied (32–37). An unusual labile lamellar structure with a collective undulation mode has been observed in the SDS/pentanol/cyclohexane/water system (32–34). These lamellae occur in the vicinity of a microemulsion phase in a phase diagram, but contain less alcohol than that needed to form isotropic microemulsions. The results of these studies emphasized the importance of interfacial fluidity for the formation of microemulsions, and suggested the role of alcohol (cosurfactant) in increasing the interfacial fluidity resulting in a transition from a periodically organized structure (lamellae) toward random isotropic microemulsions. We have investigated the phase behavior of the same system by mixing 0.4 g SDS, 5 ml cyclohexane, 1 ml 1-pentanol, and various amounts of water together. An analogous phase transition of isotropic → birefringent → isotropic → turbid was observed. The macroscopic similarity between the sodium stearate and the SDS system indicates that the solubilization and phase transition observed in Fig. 1a are probably related to the formation and stability of birefringent lamellae. This argument can be partially substantiated by the result in Fig. 1b. When the amount of pentanol decreases by one-half, the pronounced solubilization maximum observed in Fig. 1a vanishes and the birefringent region enlarges. The height of birefringent region decreases with increasing oil chain length. It is clear that the stability of lamellae is influenced by the alcohol concentration and oil chain length.

The periodic long-range orientational order of lamellae mainly results from the solute–solvent as well as the solute–solute interactions (38). The penetration of solvent (oil) molecules into the aliphatic layer of the interface (solute–solvent interaction) results in more rigid surfactant chains (7, 10, 13, 15). The cohesive interactions in the aliphatic layer are thus increased, leading to a long-range ordered and more rigid interface. This partly accounts for the observation of the birefringent phase in the short-chain oil region (C_8 to C_{12}) in Fig. 1a. Furthermore, the continuous decrease in the water solubilization in isotropic microemulsions with decreasing oil chain length from dodecane to hexane in Fig. 1a can also be explained by the increasing oil penetration (solvation effect). The oil penetration increases the packing ratio v/a_0l_c, thus decreasing the natural radius. This conjecture has been verified both experimentally (39) and theoretically (40). It has been estimated that for a surfactant

film with a v/a_0l_c value close to unity, v/a_0l_c may increase to about 1.5–2 in the presence of hexane, while it may remain unchanged in the presence of tetradecane or hexadecane (41).

The above analysis focuses on the influence of oil on the interfacial rigidity and curvature. The effect of alcohol can be analyzed in a similar way. Since many single-chain ionic surfactants have a bulky polar head group (a_0) and a relatively smaller cross-sectional area (v/l_c) in the hydrocarbon chain, the packing ratio v/a_0l_c is usually smaller than unity favoring the formation of oil-in-water droplets. It has been generally observed (31) that a minimum amount of alcohol is required to form a neat phase in a binary ionic amphiphile–water system. The addition of alcohol is expected to increase hydrocarbon chain volume v (42, 43), and may slightly decrease the area per polar head group a_0 (31, 42), thus increasing the packing ratio v/a_0l_c toward unity and leading to a structural transition from normal micelles to lamellae. However, at higher alcohol concentrations, a large increase in v, and hence in v/a_0l_c, may eventually favor the formation of an "inverted" (w/o) structure. This can explain the smaller birefringent region (with higher water solubilization in the microemulsions) in Fig. 1a containing a higher alcohol concentration than that in Fig. 1b. Moreover, the partitioning of alcohol at the interface is expected to disorder the surfactant film due to a void formation between the surfactant chains (44, 45). It has also been found that alcohol partitioning at the interface increases with increasing oil chain length (1, 4). Thus the diminishing of the birefringent region can also be reasonably explained by the increasing fluidity of the interface with increasing oil chain length and alcohol concentration.

The uptake of water and oil by lamellae is probably the main factor in determining the stability of the birefringent phase. Figure 1 shows that increasing oil chain length decreases the height (water uptake) of lamellae. It has been generally observed that a fatty acid soap forms lamellae of a nonexpanding type (31). This means that the incorporation of water in lamellae can result in a marked rise in the interfacial area per polar head group as well as a reduction in the thickness of bilayers (double hydrocarbon chain layers) (31). The intake of water by lamellae is limited to the point where the interfacial area per polar head group is about twice as great as the cross section of the amphiphilic chain ($v/a_0l_c = \frac{1}{2}$) beyond which a phase transition to a new phase will occur (31). It appears that a decreasing oil chain length can increase the water uptake by lamellae due to a preferential penetration of short-chain oils (higher value of v) as compared to hexadecane.

3. Chain length compatibility in W/O microemulsions. It may be questioned whether the pronounced solubilization maximum at dodecane observed in Fig. 1a, complying with the condition of chain length compatibility, is fortuitous. Upon decreasing the hydrocarbon chain length of the surfactant, chain length compatibility has also been observed for the sodium myristate/pentanol system (1). We have further examined a system of SDS/pentanol as shown in Fig. 2. The result is similar to that in Fig. 1 and the condition of chain length compatibility is again observed. However, when varying the chain length of alcohol, no solubilization maximum at the point of chain length compatibility was observed for the sodium stearate system containing butanol (curve 1) and hexanol (curve 3) shown in Fig. 3. We could infer that the observation of chain length compatibility in various systems is not incidental, but requires specific conditions. Both alcohol chain length and concentration appear to be important factors for the chain length compatibility effect.

It is interesting to note that when the condition of chain length compatibility is obeyed, the liquid crystalline phase always vanishes at the preferred oil chain length as shown in Figs. 1a and 2a. The following explanation is postulated. The interfacial fluidity is likely to be influenced by the degree of oil penetration (static factor) and the ease of oil removal (dynamic factor) from the interface upon the col-

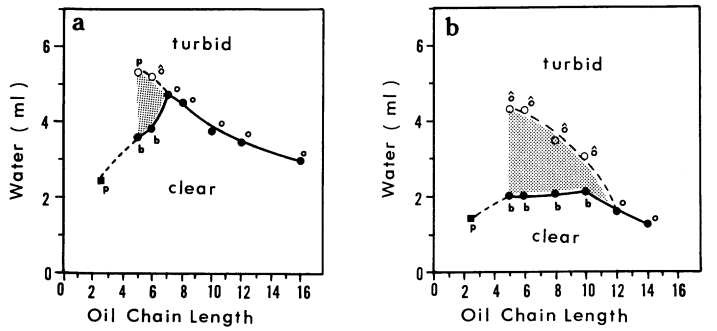

FIG. 2. Solubilization of water as a function of oil chain length in the microemulsions containing 5 ml oil, 0.7 g sodium dodecyl sulfate, and various amounts of 1-pentanol: 4 ml (a) and 1.8 ml (b). See Fig. 1 and text for other details.

lisions of droplets. Since the interpenetrable collision between microemulsion droplets is accompanied by oil removal (23), the interfacial fluidity may increase with the increasing ease of oil removal. It is likely that the environment experienced by the oil molecules residing in the aliphatic layer of interfaces is on average close to a hydrocarbon phase with an equivalent chain length of $l_s - l_a$, where l_s is the surfactant chain length, and l_a is the alcohol chain length. Any alkane shorter than $l_s - l_a$ will experience a higher average cohesive force in the aliphatic layer than that in the bulk oil phase, thus having a tendency to reside in the aliphatic layer and increasing the packing ratio as well as the rigidity of the interface. This concept involving the cohesive forces between molecules is important in light of our previous paper (2). It has been found (2) that the effect of oil on the solubilization of w/o microemulsions is dependent on the collective properties of the solvent (oil), not on the individual molecular structure of the oil. A binary alkane mixture of $C_8 + C_{16}$ can behave like C_{12} oil at the interface as far as the bulk cohesive forces are concerned, and the heterogeneity of oil chain length at the interface becomes immaterial. The result of chain length compatibility may also imply that the absorption of oil molecules into the interface (solvation effect) increases significantly for oil shorter than the preferred oil chain length. Similar absorption of alkanes in black lipid films has also been reported (15, 16).

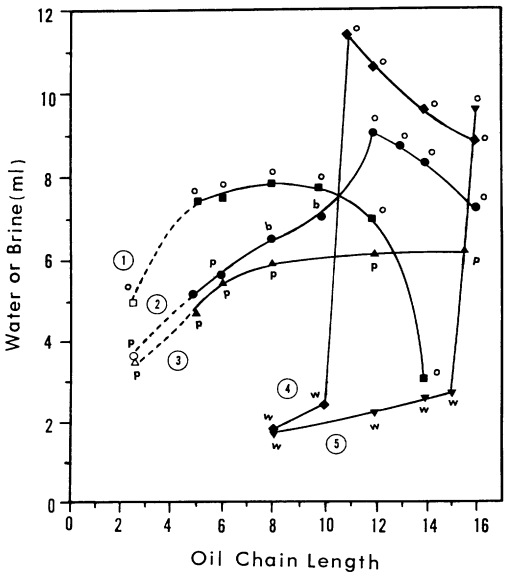

FIG. 3. Solubilization of water or brine as a function of oil chain length in the microemulsions containing 10 ml oil, 1 g sodium stearate, and 8 ml of different alcohols: 1-butanol (curve 1), 1-pentanol (curve 2), 1-hexanol (curve 3), 1-pentanol with 0.2% (w/w) sodium chloride (curve 4), and 1-pentanol with 0.25% (w/w) sodium chloride (curve 5). The open symbols at an oil chain length of 2.4 represent benzene.

The pronounced maximum of water solubilization in microemulsions with the condition of chain length compatibility can be considered a result of counteracting effects of interdroplet interactions and intradroplet in-

teractions (46). The intradroplet interaction is related to the cohesive force between adjacent hydrocarbon chains at the interface and to the rigidity of the interface. Starting from a short-chain oil, increasing the oil chain length will gradually reduce the cohesive interaction between the hydrocarbon chains of the interface and decrease the interfacial rigidity due to decreasing oil penetration. The solubilization in microemulsions thus increases due to a decrease in packing ratio v/a_0l_c and a consequent increase in natural radius (Figs. 1a and 2a). At longer oil chain lengths, the intradroplet interaction gradually diminishes (thus interfacial fluidity increases) and the attractive interdroplet interaction starts governing the system. One consequently expects a decrease in the solubilization in microemulsions with a further increase in the oil chain length. At the point of chain length compatibility, these two interactions are both minimized, hence resulting in a maximum solubilization. In Fig. 3, the interdroplet interaction dominates all the microemulsions containing butanol (curve 1), while the intradroplet interaction governs all the microemulsions containing hexanol (curve 3); hence we observe no chain length compatibility effect due to the absence of these two counteracting effects.

For some short-chain oils (C_7 or shorter) and aromatic hydrocarbons in Fig. 1a, phase separation of surfactant precipitates swollen by water occurs. In many cases, a "gel-like" phase with anisotropy was observed. It is generally known that the gel state is intermediate between a liquid crystalline state with moderately disordered hydrocarbon chains and a crystalline state with completely ordered chains (31). We postulate that the observation of gel-like precipitates is due to the stiffness of surfactant chains resulting from the large absorption of hydrocarbons at the interface. The specific interaction between aromatic hydrocarbons and polar head groups of amphiphiles (8, 10, 47, 48) further enhances the hydrocarbon absorption. It was speculated (15–17) that interfacial tension may consequently increase due to an increase in area per surfactant head group and a possible hydrocarbon–water contact.

II. Effect of Alcohols

1. Effect of alcohol chain length. As mentioned earlier, two effects emerge from decreasing alcohol chain length in a microemulsion system. First, the hard-sphere radius of droplets decreases (3, 23). Second, the interfacial fluidity increases due to a void formation in the aliphatic layer of the interfacial film (44). Both effects lead to an increase in attractive interdroplet interaction. Using fluorescence methods, Atik and Thomas (49) have indeed found a faster ion exchange between water pools of w/o microemulsions as alcohol chain length decreases, suggesting more inelastic collisions between droplets. In contrast, increasing alcohol chain length may lead to an increase in the hard-sphere radius (3, 23) and a rigid interface (50). The result of phase equilibria in Fig. 3 supports the above statement. It shows that the phase equilibria of microemulsions containing butanol are totally driven by attractive interdroplet interaction (curve 1), while for microemulsions containing hexanol, phase equilibria are all governed by rigid interfaces (curve 3) as seen by the precipitate formation. The decrease in solubilization in curve 1 from C_8 to C_{14} can be explained by the increasing attractive interdroplet interaction with increasing oil chain length, whereas the increase in solubilization in curve 3 is due to the increase in natural radius with increasing oil chain length. It appears that a small change in alcohol chain length can strongly influence the interfacial elasticity and hence the phase behavior of microemulsions.

When salt is added to the water, solubilization in the microemulsions decreases drastically in the short-chain oil region as shown in curves 4 and 5 of Fig. 3. The phase equilibria are typically of type 1, indicating that the system is governed by interfacial bending stress. Several facts can be elucidated from this result. First of all, the addition of salt can reduce the area per head group (a_0), due to the effect of charge screening. Hence the solubilization (or

natural radius) of microemulsions decreases drastically due to a large increase in v/a_0l_c. The birefringent phase also vanishes due to such an increase in v/a_0l_c. Furthermore, the rigidity constant K may also increase upon the addition of salt (51). As oil chain length increases, the water solubilization increases abruptly and shows a maximum at undecane for microemulsions containing pentanol at 0.2% (w/w) salinity in curve 4 of Fig. 3. The abrupt increase in solubilization implies that the alcohol partitioning at the interface increases abruptly at the solubilization maximum, resulting in an increase in the fluidity and natural radius of the interface. The maximum solubilization shifts toward higher oil chain length when salinity is increased from 0.2 to 0.25% in curve 5 of Fig. 3. This may be interpreted by a tighter molecular packing at the interface with higher salinity, which necessitates longer oil chain length to induce alcohol partitioning at the interface (1, 4). The proportionality between a_0 and v at fixed l_c in the packing ratio v/a_0l_c also dictates the criterion that smaller a_0 at higher salinity requires a smaller v (less oil penetration), and hence longer oil chain length to attain proper interfacial curvature and elasticity.

With regard to how the solubilization changes with alcohol chain length, Fig. 3 indicates that for microemulsions with rigid interfaces (oil chain length less than C_{10} in curves 1, 2, and 3), the water solubilization is on the order of C_5OH (0.2% salinity) < C_6OH < C_5OH < C_4OH, which increases in the direction of decreasing alcohol chain length (increasing the interfacial fluidity). In contrast, for microemulsions with fluid interfaces (oil chain length longer than C_{12} in curves 1, 2, and 4), the water solubilization is on the order of C_4OH < C_5OH < C_5OH (0.2% salinity), which increases in the direction of increasing alcohol chain length (increasing interfacial rigidity). The effect of salinity is obviously equivalent to increasing alcohol chain length. All these changes are consistent with the theory presented in part I of this series. The above discussion is based on an assumption that total interfacial area for solubilization does not change drastically with alcohol chain length; hence only the effects of natural radius and interfacial elasticity are considered.

2. *Effect of alcohol concentration.* The effect of pentanol concentration on solubilization in microemulsions containing hexadecane, dodecane, octane, and benzene is shown in Fig. 4. The solubilization shows a maximum as a function of pentanol concentration. The maximum is most pronounced for the dodecane system due to the chain length compat-

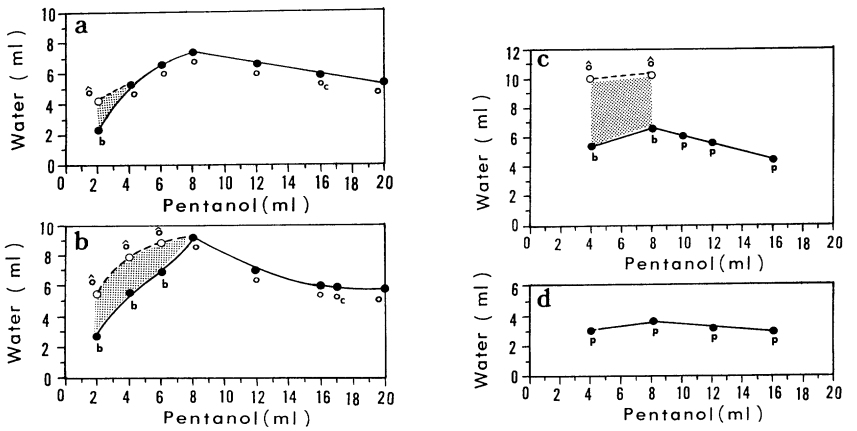

FIG. 4. Solubilization of water as a function of 1-pentanol concentration in the microemulsions consisting of 1 g sodium stearate, 1-pentanol, and 10 ml of different oils: hexadecane (a), dodecane (b), octane (c), and benzene (d). See Fig. 1 and text for other details.

ibility effect. We may infer that chain length compatibility is probably one of the necessary conditions for a system to achieve its highest possible solubilization. Increasing alcohol concentration can increase the alcohol partitioning at the interface, and consequently increase the total interfacial area for solubilization. This will contribute to an increase in solubilization. However, at sufficiently high alcohol concentration, the fluidity of the interface increases (33, 34, 45) to the extent that attractive interdroplet interaction starts dominating the system, and hence the solubilization decreases. The attractive interdroplet interaction is evidenced by the existence of a critical-like behavior (3, 52). We have found that the dodecane system containing 17 ml pentanol is close to a critical point based on the phase equilibrium of two isotropic phases with equal volumes. The critical point in microemulsions containing hexadecane was observed at about 16 ml pentanol.

Friberg and Burasczenska (46) have discussed the maximum water solubilization at a specific alcohol/surfactant ratio in terms of a diffuse electric double-layer effect in a ternary surfactant–alcohol–water system. Since the major effect of an electric double layer is on the molecular packing and the curvature of the interface, their analysis is basically in line with ours. The total alcohol/surfactant molar ratio at the maximum water solubilization in Fig. 4 is approximately 23 and is apparently independent of oil chain length.

The solubilization in microemulsions containing benzene shows no sizable change with respect to alcohol concentration (Fig. 4d). This seems to imply that alcohol does not penetrate into the interfacial film effectively. It has been generally observed that w/o microemulsions consisting of aromatic solvents always have less water solubilization than that of nonpolar solvents (e.g., alkanes) (8, 39, 47). The specific surfactant head group–solvent interaction is considered to be the cause. This specific interaction can result in a large absorption of solvent molecules into the aliphatic layer of the interface (solvation effect) and hence a greater $v/a_o l_c$ value. It is also speculated that the solvation of surfactant polar heads by the solvent molecules may hinder the partitioning of alcohol at the interface and may even raise the interfacial tension due to an increase in solvent–water contact (12, 47).

Figure 5 shows the water solubilization in microemulsions containing hexadecane as a function of surfactant concentration at constant alcohol/surfactant ratios. It has been suggested that such a plot can provide information about solubilization efficiency (amount of solubilized water per surfactant molecule) from the slope, and the amount of surfactant not partitioning at the interface from the intercept on the surfactant concen-

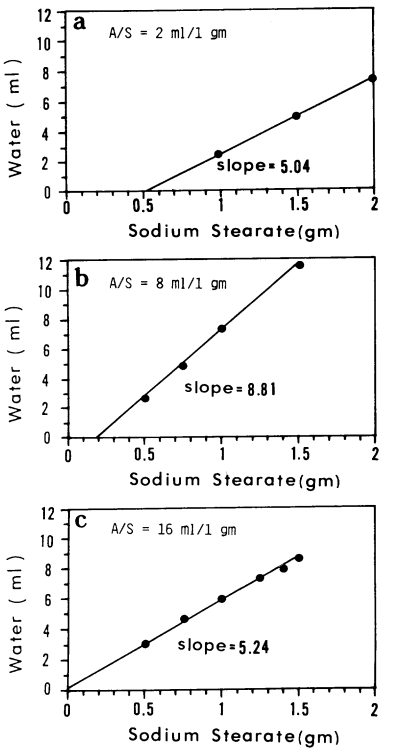

FIG. 5. Solubilization of water as a function of sodium stearate concentration in the microemulsions consisting of 10 ml hexadecane, 1-pentanol, and sodium stearate. The alcohol-to-surfactant ratio (A/S) is kept constant in each plot: 2 ml pentanol/1 g sodium stearate (a), 8 ml pentanol/1 g sodium stearate (b), and 16 ml pentanol/1 g sodium stearate (c).

tration axis (50, 53, 54). The result in Fig. 5 indicates that the solubilization efficiency of hexadecane microemulsions is maximum at a ratio of 8 ml pentanol/1 g sodium stearate. A maximum water solubilization at this ratio has been reported in Fig. 4a. However, the maximum solubilization efficiency does not correspond to a maximum partitioning of surfactant at the interface as previously reported (50, 53, 54). Instead, the result indicates that the total interfacial area, which is proportional to both surfactant and alcohol partitioning at the interface, keeps increasing with increasing alcohol/surfactant ratio, despite the decrease in solubilization efficiency. This result suggests that the solubilization efficiency of microemulsions may not always be proportional to the total interfacial area in the microemulsions. The curvature and elasticity of the interface are probably more decisive factors for solubilization.

The linearity in the plots of Fig. 5 implies a constant interfacial composition of microemulsion droplets when the alcohol/surfactant ratio is kept constant. Thus the droplet size may not change; only the number density of microemulsion droplets increases with total emulsifier concentration. The linearity of the plots further suggests that the interdroplet attractive force does not change with the number density of droplets in the solution, but mainly depends on interfacial curvature (droplet size) and elasticity.

III. Effect of Salinity

1. Optimal salinity in single-phase W/O microemulsions. Figure 6a shows the brine solubilization as a function of salinity in microemulsions containing isobutyl alcohol (IBA), sodium stearate, and dodecane. A maximum brine solubilization was observed at the salinity of 1.5%. We shall refer to this salinity as an "optimal salinity" (55). The maximum brine solubilization is the result of counteracting effects of attractive interdroplet interaction and interfacial bending stress. The decreasing brine solubilization with increasing salinity is due to an increase in interfacial rigidity and geometric ratio $v/a_0 l_c$ with increasing salinity. A decreasing alcohol partitioning at the interface with increasing salinity may also contribute to the decrease in brine solubilization (55, 56) due to a decrease in total interfacial area. In the low salinity region, the increase in brine solubilization with increasing salinity can be explained by the increasing alcohol partitioning at the interface (55). This enhanced alcohol partitioning may be attrib-

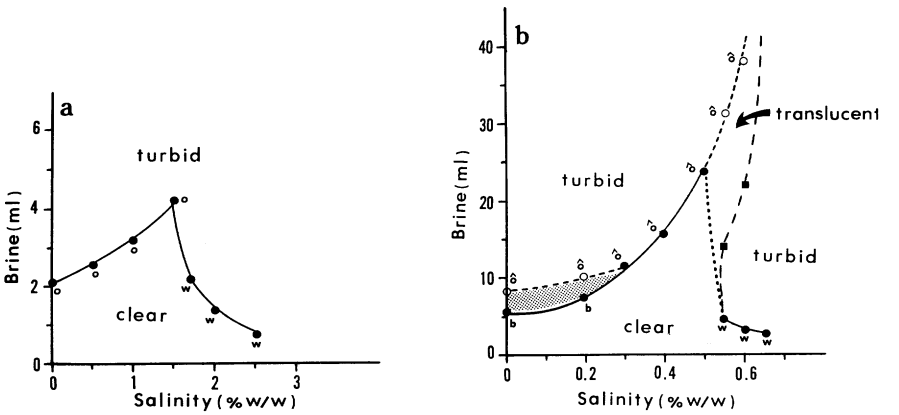

FIG. 6. Solubilization of brine as a function of salinity in the microemulsions consisting of 10 ml dodecane, 1 g sodium stearate, and 4 ml of different alcohols: isobutyl alcohol (a) and 1-pentanol (b). The filled circles represent the first boundary and the open circles represent the second boundary. The filled squares represent the boundary of transition from turbid to the second isotropic phase. An imaginary dotted line has been drawn between the first isotropic and the second isotropic region.

uted to the salting-out effect (57). The addition of salt also reduces the attractive interaction of fluid interfaces (58), and hence increases the solubilization.

The term "optimal salinity" was originally defined as the salinity at which a middle-phase microemulsion solubilizes equal amounts of oil and brine (59, 60). The existence of middle-phase microemulsions in equilibrium with excess oil and brine has been attributed to both attractive interdroplet interaction and interfacial bending stress (38, 61). The reason for our designation of this terminology to a single-phase microemulsion system is self-explanatory when we examine the result of phase equilibria shown in Fig. 6a. Upon addition of excess brine, a microemulsion in equilibrium with oil (type 2 phase equilibrium) was observed for salinity less than or equal to the optimal salinity (1.5%), while a microemulsion in equilibrium with brine (type 1 phase equilibrium) was observed for a salinity of 2.5% and higher. Only at the salinities of 1.7 and 2% was a transition of two-phase (type 1) to three-phase (coexistence of type 1 and type 2) and then to two-phase (type 2) equilibria observed upon continuous addition of excess brine. The three-phase equilibrium occurs in the vicinity of optimal salinity where the driving force for phase separation changes from attractive interdroplet interaction to interfacial bending stress. This corroborates the view that three-phase equilibria are driven by both interdroplet interaction and interfacial bending stress.

When IBA was replaced by pentanol, a strange phase behavior was observed as shown in Fig. 6b. Only two-phase equilibria were observed in all samples, and a narrow, bluish, translucent single-phase region was observed where three-phase equilibria would have been anticipated according to Fig. 6a. This single phase is analogous to the second isotropic phase observed in the AOT system (29, 30). The reason for this observation is not clear. A comparison between Figs. 6a and 6b seems to indicate that it is related to the vanishing of three-phase equilibria as a result of the increase in alcohol chain length. Since increasing alcohol chain length can reduce the attractive interdroplet interaction, a clear isotropic microemulsion may exist when the interfacial bending stress has already diminished, but the interdroplet interaction is not strong enough to induce phase separation. Further, a possible continuous phase inversion from w/o to o/w structure may occur in the second isotropic region. Similar second isotropic regions are found in most pentanol microemulsions presented in Figs. 7 and 8. However, they are not shown in the figures for clarity and simplicity.

2. Effects of alcohol and oil on optimal salinity. As alcohol chain length increases from IBA to pentanol, the optimal salinity decreases as shown in Fig. 6. If we consider that the role of salinity is to promote the interfacial rigidity and increase the packing ratio v/a_0l_c (decrease the natural radius) of w/o microemulsions, the salinity required by pentanol microemulsions should be lower than that by IBA microemulsions due to higher interfacial rigidity and packing ratio of microemulsions containing pentanol.

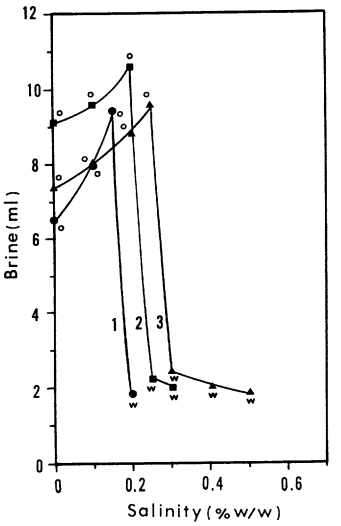

FIG. 7. Solubilization of brine as a function of salinity in the microemulsions consisting of 1 g sodium stearate, 8 ml 1-pentanol, and 10 ml of different oils: octane (curve 1), dodecane (curve 2), and hexadecane (curve 3). Only the first isotropic region is reported.

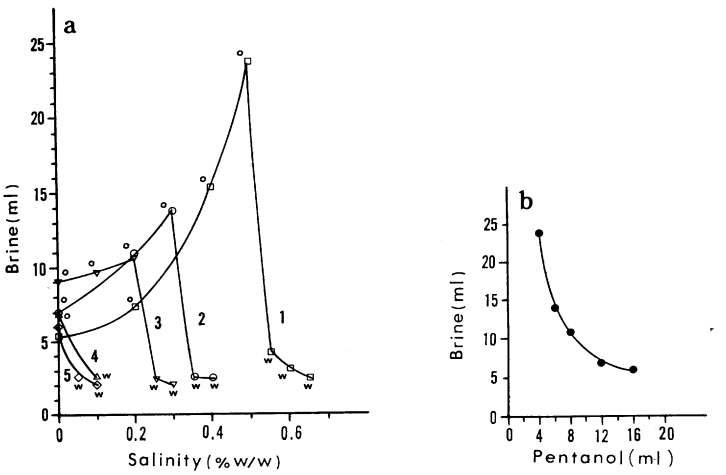

FIG. 8. (a) Solubilization of brine as a function of salinity in the microemulsions consisting of 10 ml dodecane, 1 g sodium stearate, and different amounts of 1-pentanol: 4 ml (curve 1), 6 ml (curve 2), 8 ml (curve 3), 12 ml (curve 4), and 16 ml (curve 5). (b) A plot of the maximum solubilization of each curve in (a) as a function of 1-pentanol concentration.

Figure 7 shows that, as oil chain length increases, the optimal salinity increases. This can be explained by the increasing fluidity and the decreasing v/a_0l_c of the interface with increasing oil chain length. Thus, higher salinity is required to make a rigid interface and to decrease the natural radius.

Figure 8a shows that the optimal salinity decreases with increasing alcohol concentration. At very high alcohol concentrations, the brine solubilization directly decreases upon the addition of salt (optimal salinity = 0). The addition of alcohol increases the polarity of the oil phase, which in turn will increase the solvent (both alcohol and oil molecules) penetration into the aliphatic layer of the interface and thus decrease the optimal salinity due to higher packing ratio v/a_0l_c. Huh (17) has also concluded similarly that alcohol increases the solubility of surfactant in the oil phase, resulting in a better interaction between surfactant chains and oil molecules.

As plotted in Fig. 8b, the maximum brine solubilization at optimal salinity for each curve reported in Fig. 8a decreases with increasing amounts of alcohol. Each point in Fig. 8b represents the maximum solubilization achievable for a specific system in Fig. 8a. The result of Fig. 8b implies that the addition of both salt and alcohol (cosurfactant) to a microemulsion is essential for achieving its largest possible solubilization. Though the addition of alcohol can decrease the interfacial tension and increase the total interfacial area, only a small amount of alcohol is desirable due to its negative influence on interfacial curvature and elasticity for solubilization at high alcohol concentrations. The optimal salinity serves to drive more alcohol to the interface, thus providing more interfacial area for solubilization, and to maintain an optimal interfacial rigidity and curvature in order to minimize the interdroplet interaction. It is interesting to point out that all the above-reported effects of alcohol and oil on the optimal salinity in single-phase w/o microemulsions are in agreement with those in middle-phase microemulsions (17, 62).

CONCLUSIONS

Both theoretical and experimental aspects of solubilization and phase equilibria of w/o microemulsions have been studied. A simple phenomenological approach has been applied

to the theory and the interpretation of experimental results by considering two phenomenological parameters, namely the spontaneous curvature and elasticity of interfaces. All the experiments presented are designed to elucidate how the molecular structure of various components of microemulsions influences these two parameters and hence the solubilization and phase equilibria of microemulsions. The results can be recapitulated as follows.

i. Oil can influence the property of an interface through a surfactant chain–oil interaction. Strong interaction leads to a large penetration of oil molecules into the surfactant chain layer (solvation), thus increasing the rigidity and curvature (or packing ratio v/a_0l_c) of the interface. Oil molecules with a small molecular volume or high polarity often produce strong solvation effects on the interface.

ii. Alcohol (cosurfactant) is essential in promoting interfacial fluidity for the formation of microemulsions. Decreasing the alcohol chain length can increase the interfacial fluidity and hence the attractive interdroplet interaction. On the other hand, increasing the alcohol chain length often increases the rigidity and curvature of the interface. For alcohols which promote interfacial fluidity, increasing alcohol partitioning at the interface can increase the natural radius and fluidity of the interface.

iii. There exists an optimal salinity for a given w/o microemulsion at which maximum brine solubilization occurs. The addition of salt usually leads to tighter molecular packing at the interface and a decrease in natural radius. For salinity lower than the optimal salinity, these effects together with salting-out effects tend to increase the solubilization. However, for salinity higher than optimal salinity, it increases the interfacial rigidity and curvature, thus decreasing the solubilization.

All the above principles constitute the basis of a self-consistent interpretation of our experimental results. The implications of this study are important. Some fundamental guidelines for the formulation of w/o microemulsions are proposed as follows.

i. The solubilization of a microemulsion is determined by the curvature and elasticity of the interface, as well as the total interfacial area. At constant total interfacial area, the solubilization is proportional to the radius of droplets. At a given surfactant concentration, the maximum solubilization efficiency of the system can be achieved by adjusting the interfacial curvature and elasticity to optimal values at which the bending stress and the attractive force of the interface are both minimized. Hence, one can increase the solubilization of a microemulsion with a rigid interface by increasing its natural radius and fluidity of the interface. On the other hand, the solubilization of a microemulsion with a fluid interface can be increased by increasing its interfacial rigidity and decreasing the natural radius.

ii. The study of phase equilibria of microemulsions can serve as a direct measure to assess the property of the interface and the driving force for phase separation. Knowing the cause of the instability of microemulsion droplets is the first step in the formulation of microemulsions. One often observes a w/o microemulsion with a highly curved and relatively rigid interfacial film in equilibrium with excess water at the solubilization limit due to interfacial bending stress. The solubilization in this microemulsion is limited by the natural radius of the interface. On the other hand, a microemulsion can coexist in equilibrium with an excess oil phase containing a low density of microemulsion droplets due to attractive interdroplet interaction when the interface is highly fluid. In this case, the solubilization is determined by the stability of the droplets. Sometimes a birefringent phase will occur if the interface is rigid with an intermediate value of v/a_0l_c (close to 1).

iii. When phase separation of microemulsions is driven by the bending stress of a rigid interface, increasing the natural radius or fluidity of the interface by increasing oil chain

length, decreasing alcohol chain length, increasing alcohol/surfactant ratio, or decreasing electrolyte concentration can increase the solubilization. Among all the factors, alcohol chain length appears to be the most decisive factor in determining the basic property of the interfacial film.

iv. In contrast, when the phase separation of microemulsions is driven by attractive interdroplet interaction, increasing interfacial rigidity and decreasing the natural radius by decreasing oil chain length, increasing alcohol chain length, decreasing alcohol/surfactant ratio, or increasing electrolyte concentration can stabilize the microemulsion droplets and increase the solubilization.

v. The addition of alcohol (cosurfactant) can increase the total interfacial area at low alcohol concentrations, thus increasing the solubilization. But at high alcohol concentrations, phase separation occurs at a smaller droplet size due to the increase in attractive interdroplet interaction. Hence, only an optimal amount of alcohol is desired to formulate a microemulsion with maximum solubilization capacity.

vi. For a given w/o microemulsion, there exists an optimal salinity at which maximum brine solubilization occurs. The maximum solubilization results from the counteracting effect of interfacial bending stress of rigid interfaces and attractive interdroplet interaction of fluid interfaces. The optimal salinity decreases with increasing alcohol chain length and concentration, but increases with increasing oil chain length.

vii. Addition of an optimal amount of alcohol and salinity together with the effect of chain length compatibility may lead to the largest possible solubilization of a given w/o microemulsion.

ACKNOWLEDGMENTS

We acknowledge the National Science Foundation (Grant NSF-CPE 8005851) for supporting this research. We are also grateful for support from the Alcoa foundation, Aluminum Company of America, Pennsylvania.

REFERENCES

1. Bansal, V. K., Shah, D. O., and O'Connell, J. P., *J. Colloid Interface Sci.* **75,** 462 (1980).
2. Leung, R., Shah, D. O., and O'Connell, J. P., *J. Colloid Interface Sci.* **111,** 286, (1986).
3. Cazabat, A. M., Langevin, D., Meunier, J., and Pouchelon, A., *Adv. Colloid Interface Sci.* **16,** 175 (1982).
4. Roux, D., Bellocq, A. M., and Bothorel, P., *Prog. Colloid Polym. Sci.* **69,** 1 (1984).
5. Huang, J. S., "Critical Phenomena in Microemulsions," tutorial lecture in 189th ACS National Meeting, Division of Colloid and Surface Chemistry, paper No. 81, April 28–May 3, Miami, 1985.
6. Robinson, B. H., Fletcher, P. D. I., McDonald. J. A., and Galal, M. F., "Neutron and Light Scattering Studies of Microemulsions," paper (No. 26) presented in 189th ACS National Meeting, Division of Colloid and Surface Chemistry, April 28–May 3, Miami, 1985.
7. Atik, S. S., and Thomas, J. K., *Chem. Phys. Lett.* **79,** 351 (1981).
8. Magid, L. J., and Martin, C. A., *in* "Reverse Micelles: Biological and Technological Relevance of Amphiphilic Structures in Apolar Media" (P. L. Luisi and B. E. Straub, Eds.), p. 181. Plenum, New York, 1984.
9. Friberg, S. E., Christenson, H., Bertrand, G., and Larsen, P. W., in "Reverse Micelles: Biological and Technological Relevance of Amphiphilic Structures in Apolar Media" (P. L. Luisi and B. E. Straub, Eds.), p. 105, Plenum, New York, 1984.
10. Maitra, A., Vasta, G., and Eicke, H. F., *J. Colloid Interface Sci.* **93,** 383 (1983).
11. Requena, J., Brooks, D. E., and Haydon, D. A., *J. Colloid Interface Sci.* **58,** 26 (1977).
12. Word, A. J. I., Rananavare, B., and Friberg, S. E., paper (No. 173) presented in 189th ACS National Meeting, Division of Colloid and Surface Chemistry, April 28–May 3, Miami, 1985.
13. Gruen, D. W. R., and Haydon, D. A., *Pure Appl. Chem.* **52,** 1229 (1980).
14. McIntosh, T. J., Simon, S. A., and MacDonald, R. C., *Biochim. Biophys. Acta* **597,** 445 (1980).
15. Gruen, D. W. R., *Biophys. J.* **33,** 149 (1981).
16. Gruen, D. W. R., and Haydon, D. A., *Biophys. J.,* 167 (1981).
17. Huh, C., *Soc. Pet. Eng. J.* Oct., 829 (1983).
18. Cazabat, A. M., Langevin, D., Meunier, J., and Chatenay, D., *in* "Macro- and Microemulsions: Theory and Applications," (D. O. Shah, Ed.), Vol. 272, p. 75. ACS symposium series, 1985.
19. Fletcher, P. D. I., Robinson, B. H., Bermejo-Barrera, F., and Oakenfull, D. G., *in* "Microemulsions" (I. D. Robb, Ed.), p. 221. Plenum, New York, 1982.
20. Auvray, L., *J. Phys. Lett.* **46,** 163 (1985).

21. Brunetti, S., Roux, D., Bellocq, A. M., Fourche, G., and Bothorel, P., *J. Phys. Chem.* **87,** 1028 (1983).
22. Roux, D., Bellocq, A. M., and Bothorel, P., *Prog. Colloid Polym. Sci.* **69,** 1 (1984).
23. Lemaire, B., Bothorel, P., and Roux, D. *J. Phys. Chem.* **87,** 1023 (1983).
24. "Cell Surface Dynamics: Concepts and Models" (A. S. Perelson, C. DeLisi, and F. W. Wiegel, Eds.), p. 468. Dekker, New York, 1984.
25. Napper, D., "Polymeric Stabilization of Colloidal Dispersions," Academic Press, New York, 1983.
26. Shah, D. O., and Hamlin, R. M., Jr., *Science* **171,** 483 (1971).
27. Senatra, D., and Giubilaro, G., *J. Colloid Interface Sci.* **67,** 448 (1978).
28. Senatra, D., and Gambi, C. M., "Surfactants in Solution" (K. L. Mittal and B. Lindman, Eds.), Vol. 3, p. 1709. Plenum, New York, 1984.
29. Frank, S. G., and Zografi, G., *J. Colloid Interface Sci.* **29,** 27 (1969).
30. Eicke, H. F., Kubik, R., Hasse, R., and Zschokke, I., "Surfactants in Solution," (K. L. Mittal and B. Lindman, Eds.), Vol. 3, p. 1533. Plenum, New York, 1984.
31. Ekwall, P., *in* "Advances in Liquid Crystals" (G. H. Brown, Ed.), Vol. 1, p. 1. Academic Press, New York, 1975.
32. Di Meglio, J. M., Dvolaitzky, M., Ober, R., and Taupin, C., *J. Phys. Lett.* **44,** 229 (1983).
33. Di Meglio, J. M., Dvolaitzky, M., and Taupin, C., *J. Phys. Chem.* **89,** 871 (1985).
34. Di Meglio, J. M., Dvolaitzky, M., Leger, L., and Taupin, C., *Phys. Rev. Lett.* **54,** 1686 (1985).
35. Miller, C. A., Ghosh, O., and Benton, W. J., *Colloids Surf.* **19,** 197 (1986).
36. Marignan, J., Delichere, A., and Larche, F. C., *J. Phys. Lett.* **44,** 609 (1983).
37. Fontell, K., Hernqvist, L. Larsson, K., and Sjoblom, J., *J. Colloid Interface Sci.* **93,** 453 (1983).
38. De Gennes, P. G., and Taupin, C., *J. Phys. Chem.* **86,** 2294 (1982).
39. Peri, J. B., *J. Colloid Interface Sci.* **29,** 6 (1969).
40. Mukherjee, S., Miller, C. A., and Fort, T., *J. Colloid Interface Sci.* **91,** 223 (1983).
41. Angel, L. R., Evans, D. F., and Ninham, B. W., *J. Phys. Chem.* **87,** 538 (1983).
42. Friberg, S. E., *Prog. Colloid Polym. Sci.* **68,** 41 (1983).
43. Wennerstorm, H., *J. Colloid Interface Sci.* **68,** 589 (1979).
44. Shibata, T., Sugiura, Y., and Iwayanagi, S., *Chem. Phys. Lipids* **31,** 105 (1982).
45. Lufimpadio, N., Nagy, J. B., and Derouane, E. G., "Surfactants in Solution" (K. L. Mittal and B. Lindman, Eds.), Vol. 3, p. 1483. Plenum, New York, 1984.
46. Friberg, S. E., and Burasczenska, I., *Prog. Colloid Polym. Sci.* **63,** 1 (1978).
47. Keh, E., and Valeur, B., *J. Colloid Interface Sci.* **79,** 465 (1981).
48. Chaiko, M. A., Nagarajan, R., and Ruckenstein, E., *J. Colloid Interface Sci.* **99,** 168 (1984).
49. Atik, S. S., and Thomas, J. K., *J. Phys. Chem.* **85,** 3921 (1981).
50. Bansal, V. K., Chinnaswamy, K., Ramachandran, C., and Shah, D. O., *J. Colloid Interface Sci.* **72,** 524 (1979).
51. Ober, R., and Taupin, C., *J. Phys. Chem.* **84,** 2418 (1980).
52. Roux, D., and Bellocq, A. M., *in* "Macro- and Microemulsions: Theory and Applications," (D. O. Shah, Ed.), Vol. 272, p. 105. ACS symposium series, 1985.
53. Pithapurwala, Y., Ph.D. thesis, University of Florida, 1984.
54. Johnson, K. A. and Shah, D. O., *in* "Surfactant in Solution" (K. L. Mittal and P. Bothorel, Eds.), Vol. 6, p. 1441. Plenum, New York, 1986.
55. Pithapurwala, Y. K., and Shah, D. O., *Chem. Eng. Commun.* **29,** 101 (1984).
56. Chou, S. I., and Shah, D. O., *J. Colloid Interface Sci.* **80,** 49 (1981).
57. Beunnen, J. A., and Ruckenstein, E., *Adv. Colloid Interface Sci.* **16,** 201 (1982).
58. Bedwell B., and Gulari, E., *J. Colloid Interface Sci.* **102,** 88 (1984).
59. Healy, R. N., Reed, R. L., and Stenmark, D. G., *Soc. Pet. Eng. J.,* 147, June, 1976.
60. Chan, K. S., and Shah, D. O., SPE 7896, presented at "SPE-AIME International Symposium on Oilfield and Geothermal Chemistry Meeting, Houston, TX, June, 1979."
61. Safran, S. A. and Turkevich, L. A. *Phys. Rev. Lett.* **50,** 1930.
62. Hsieh, W. C., and Shah, D. O., SPE 6594, presented at "SPE-AIMR International Symposium on Oil field and Geothermal Chemistry Meeting, La Jolla, CA, June, 1977."